LUND UNIVERSITY

Comparison of IMRT delivery techniques and helical Tomo Therapy using Pareto front evaluation

Master of Science Thesis

Hunor Benedek

Supervisors: **Crister Ceberg [1], Per Engström [2], Tommy Knöös [2], Anna Karlsson [3] and Claus Behrens [3]**

1 : Lund University, Medical Radiation Physics, Clinical Sciences, Lund , Sweden
2 : Lund University Hospital, Radiation Physics, Lund, Sweden
3 : Copenhagen University Hospital Herlev, Division of Radiotherapy, Herlev, Denmark

Abstract

Purpose: The purpose of this work was to explore the possibility to compare treatment-planning- and treatment-delivery systems for intensity modulated radiation therapy (IMRT) using an objective approach. The approach investigated was the Pareto front concept. An additional aim was to adequately compare three different IMRT treatment planning and delivery systems

Materials and methods: In IMRT treatment planning the goal is to find an optimal compromise between organ at risk (OAR) sparing and target coverage. During the optimization process objectives are chosen for each OAR and for the planning target volume (PTV). For a Pareto optimal plan one objective cannot be improved without worsening another objective. This makes IMRT optimization suitable for Pareto front evaluation. A set of Pareto optimal plans form a Pareto front. By using Pareto front evaluation the influence of individual plans is suppressed and the whole range of plans with the chosen objectives can be evaluated at the same time. Pareto fronts from different treatment planning systems (TPSs) are expected to differ from each other. In this study, different head and neck cases were used. Several plans with varying importance concerning the sparing of a specific OAR were created for each case using different TPSs. The importance of the PTV coverage was held constant for all plans. The TPSs used in the study were Oncentra Masterplan (OMP) (Nucletron B.V.), Eclipse (Varian Medical Systems) and TomoTherapy (Tomotherapy inc.) planning system. A Pareto front was obtained for each TPS by plotting the average OAR dose as a function of underdosed volume of the PTV. The underdosed volume was defined as the relative volume that receives less than 95% of the prescribed dose. Each plan fulfilled the dose restrictions for OARs according to the clinical protocol used apart from the OAR chosen for the trade-off.

Results: The TomoTherapy Pareto front is situated below both the OMP front and the Eclipse front indicating that for the same target coverage, the sparing of the parotid is always favourable for this technology. For low priority OAR sparing, however, the Eclipse and the TomoTherapy fronts exhibit almost equal target coverage. As the importance of the OAR increases the target coverage decreases faster for the Eclipse front compared to the TomoTherapy front and is approaching the same coverage as OMP.

Conclusion: The results clearly indicate that the approach of using Pareto fronts for different systems is a feasible way to compare different methods and technologies for advanced radiotherapy. For the particular cases studied, TomoTherapy seems to be superior to OMP and Eclipse regarding target coverage and sparing of the parotid gland.

Contents

1 Introduction

This Master's Thesis Project was carried out at the Radiation Physics department at Lund university hospital in collaboration with Herlev Hospital, Denmark.

1.1 Background

Radiation therapy is a very common modality to treat cancer generally and head and neck cancer particularly [1, 2]. After surgery radiation therapy is the most effective treatment for cancer [2]. Patients with locally advanced, stage 3 or 4 disease, require a combination of chemotherapy and radiation therapy or surgery. Patient with early stage head and neck cancer are often treated with either surgery or radiation therapy [1].

Head and neck tumours are often situated close to critical organs at risk (OAR). Because of this, obtaining a high cure rate while preserving organs at risk becomes challenging. The function of risk organs are often affected by both the cancer tumour and the treatment [1]. Organs at risk that often come into conflict with the tumours are the spinal cord, brain stem, the optical apparatus, and the salivary glands. Some of these organs are considered to be vital and are therefore not negotiable regarding maximum dose. Other organs are not vital and can be sacrificed in order to achieve better tumour control [3]. Tumour control, or Tumour Control Probability (TCP), is a commonly used model to estimate the biological effect of the irradiated volume of the tumour. Large TCP corresponds to higher cure rate. Tumour control is strongly dose dependent. Even a small underdosed tumour volume can lead to a significant loss in tumour control probability [4].

Nonvital organs, e.g. the parotid salivary glands, often lose their function due to radiation therapy. The parotid glands produce 60%-65% of the total saliva and are very radiation sensitive [5, 6]. Xerostomia is therefore the most common side effect of radiation therapy in the head and neck region. Not only is the saliva production reduced by the radiation but also the viscosity, the concentration of minerals and proteins, and pH in the saliva are affected [5]. Studies have shown that full or partial recovery of saliva production is possible over time if the average dose to the parotid is lower than a threshold of 26 gray (Gy) [6]. The consequence for the patient can be worsened ability to swallow, chew and talk. Most patients need to change their diet in order to cope with the xerostomia.

The publication from Anders Brahme and colleagues at the Karolinska Institute in Stockholm in 1982 is considered to be the starting point for Intensity modulated radiation therapy (IMRT) by numerous articles [7, 8]. Brahme et al. showed that, by rotating a modulated beam profile, it was possible to generate a ring of uniform dose around a blocked circular centre [9]. This paper also showed the possibility to start with the desired dose and calculate a non uniform fluence required to generate it. This process is today called inverse planning or optimization.

Today IMRT is the state of the art in radiation therapy and in particular Helical Tomo Therapy which combines modulated beam profiles and rotation, referred to as rotational IMRT (RIMRT). Other IMRT techniques are using a number of pre-set beams with modulated fluence. These techniques are called standard IMRT (SIMRT).

It has been shown that IMRT is superior to 3D conformal radiation therapy for complex H&N cancers such as bilateral lymph node involvement. It is also shown that IMRT, by its ability to generate concave dose distributions, can improve the protection of the salivary glands [10-15].

Different IMRT treatment planning systems (TPS) have previosly been evaluated and compared. However, accomplishing an objective study has shown to be difficult. The ultimate goal is an objective approach that evaluates the entire clinical chain. Earlier studies compare single treatment plans from the different systems, often by comparing the dose volume histograms (DVH) [16-22]. By comparing single plans only the plans themselves are compared and not the entire system.

1.3 Optimization

The optimization begins with assigning objectives in agreement with the dose prescriptions. These objectives are called Dose Volume Objectives (DVO). There are various types of DVOs such as Maximum Dose, Minimum Dose, and volume based objectives. There are some differences between the three treatment planning systems regarding the DVOs which will be described later in this thesis. The DVOs are assigned to important critical structures, OARs, and outlined tumour structures. Every DVO is also ranked relative to the others by assigning an importance or weighting factor. The goal of the optimization is to accomplish a dose distribution defined by the DVOs. To measure the difference between the desired dose and the actual dose the optimization algorithm needs an objective function or cost function. The objective function needs to express the voxel by voxel deviation from the desired dose including the importance assigned in the DVO. An objective function often used is the weighted sum of the difference between the desired and the actual dose for each voxel. The desired dose to the *i*th voxel is denoted as d_i^{des} and the actual dose as d_i. A general form of the objective function then can be formulated as:

$$cost = \sum_{i=1}^{N} s_i \left(d_i - d_i^{des}\right)^2 \qquad (1)$$

Were *N* is the number of voxels considered and s_i is the importance assigned to voxel *i*.
The goal of the optimization is to minimize the sum of all individual objective functions. This can be done using two categories of optimization algorithms, deterministic and stochastic. A common used deterministic method is the *gradient descend* method.
Every beam is divided into smaller beams called beamlets. The beamlets correspond to the projection of the PTV for the given beam. Every bemalet is traced from the source through the patient. The beamlets are then weighted. The optimization engine, the algorithm that drives the optimization forward, alters the beamlet weights in a deterministic way. The idea of the gradient method is to calculate the changes in beamlet weights in order to minimize the objective function. The changes in beamlet weights can be arrived at via the first and the second derivative of the objective function. The change in weight for beamlet *j* for a given iteration can be written as:

$$\Delta w_j = -\alpha \left(\frac{dF}{dw_j} \Big/ \frac{d^2F}{dw_j^2} \right) \qquad (2)$$

α is a damping factor to make sure that the function converges to a solution. Using equation 2 the change in beamlet weights regarding the DVOs becomes:

$$\Delta w_j = -\alpha \frac{\sum_{i=1}^{N} s_i \left(d_i - d_i^{des}\right) D_{ij}}{\sum_{i=1}^{N} s_i D_{ij}^2} \qquad (3)$$

The weight change is an average of the dose difference for all the voxels affected by the beamlet. The average is dependent on the importance, s_i, assigned by the DVOs. Only changes that improve the objective function are accepted. As the optimization runs the change in beamlet weights are calculated for every iteration, until a plateau is reached. In other words the optimizer cannot find a better solution and the optimization is ceased by the user or by a stopping criteria.
The most common stochastic method is called simulated annealing. As opposed to the gradient method simulated annealing can accept an increase in the objective function with a probability of $e^{(-\Delta cost\,/kT)}$ where k is the Boltzman constant and T is the temperature. In the beginning of the optimization T is set high so that large increases in the objective function are accepted. As the iterations proceeds T is reduced and at the end of the optimization no increase is accepted. The stochastic methods can escape local minima by accepting increases in the objective function. The gradient methods are a lot faster than stochastic methods[23].

The optimization often has to deal with contradictory objectives. For example, as mentioned above, the parotid gland and the PTV often overlap or are close to each other. A compromise or trade off between the objectives is necessary. To deal with contradicting objectives the DVO for the parotid gland is assigned a lower importance which makes the other more, important structures more dominant in the objective function. A mathematical framework to express a trade-off, such as the one for contradicting objectives, is the concept of Pareto optimality. The Pareto concept is described in detail in section 1.5[24].

1.4 Segmentation and final dose calculation

The optimization described above only calculates the mathematically optimal fluence. This fluence cannot be delivered by any linear accelerator. In order to deliver the optimal fluence the treatment plan has to be segmented. The segmentation algorithm converts the optimal fluence to physically deliverable fluence by utilizing the multi leaf collimators (MLC) to modulate the beam. The dose can be delivered by two different MLC segmentations for SIMRT, the step & shot technique and dynamic delivery technique[25].

The step & shot technique uses a number of small segments formed by the MLC. These small segments have different size and intensities together adding up to the total fluence. The radiation is off during the motion of the MLC leafs[26].

The dynamic delivery technique forms a slit with the two MLC banks. The slit is then moved from one side of the PTV to the other. The radiation is on during the movement and it is the leaf speed that modulates the beam.

The segmentation often worsens the treatment plan because of the physical and technical limitations of the MLC. For example the MLC cannot move infinitely fast, the MLC leaves have a thickness and therefore the resolution is not optimal. To account for this loss in quality some TPSs have incorporated the physical characteristics of the MLC in the optimization. Then segmentation is made for each iteration saving time for the treatment planner.

After the segmentation a final dose calculation including a full scatter calculation is needed. The dose calculation algorithm uses the segmented fluence to calculate the absorbed dose in the patient.

1.5 The Pareto front concept

A solution, x, is *Pareto optimal* if and only if it is feasible and

$$\left(f_0(x)-K\right)\cap \mathrm{O} = \left\{f_0(x)\right\} \qquad (4)$$

Where O is a set of achievable values, $\left(f_0(x)-K\right)$ the set of values that are better than or equal to $f_0(x)$ i.e. the only feasible value better than or equal to $f_0(x)$ is $f_0(x)$ itself. This is illustrated in figure 1. The grey area in figure 1 is the set of feasible values, O. The solid line consists of Pareto optimal solutions. The dashed line is the border between feasible and not feasible solutions but there are no Pareto optimal solutions[27].
If multiple Pareto optimal solutions do exist, there is a conflict between the objectives. A *Pareto optimal* solution is equivalent with the fact that one objective cannot be improved without worsening at least one other.

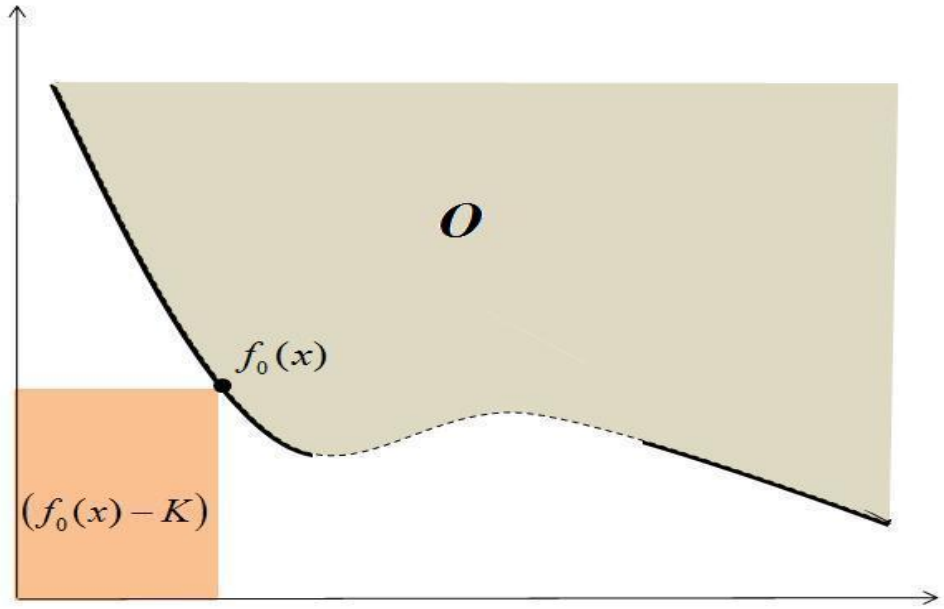

Figure 1: [27] The figure illustrates a feasible set of objective values, *O*, with two contradicting objectives (gray area). Each axis represents an objective. The point $f_0(x)$ is a Pareto optimal solution if there is no feasible solution in the orange area, $(f_0(x)-K)$. The solid line consists of Pareto optimal solutions. The dashed line is the boundary between feasible and non feasible solutions but no Pareto optimal solutions exist.

Concerning the IMRT process a set of Pareto optimal solutions is represented by a set of treatment plans that fulfils the dose planning goals [24, 28]. A set of Pareto optimal solutions sample a Pareto front. For IMRT the Pareto fronts can be visualized by plotting the contradicting objectives as shown in figure 2. Pareto fronts from different systems may differ from each other and make a comparison possible. By comparing Pareto fronts instead of single treatment plans

the influence of one plan is reduced and a whole range of plans can be evaluated at the same time. In an earlier study the possibility of comparing different treatment strategies with the same system is investigated[29]. In that study the idea of comparing different treatment planning and delivery systems using Pareto fronts was presented. Another use of the Pareto fronts in IMRT is the so called Pareto navigation. The Pareto navigation aims to find the best compromise between the objectives. This is made by automatically generation a large number of Pareto optimal plans and then choosing the most favourable[30]. Other studies have used Pareto optimal fronts for investigating trade-offs in IMRT treatment plans [31-33].

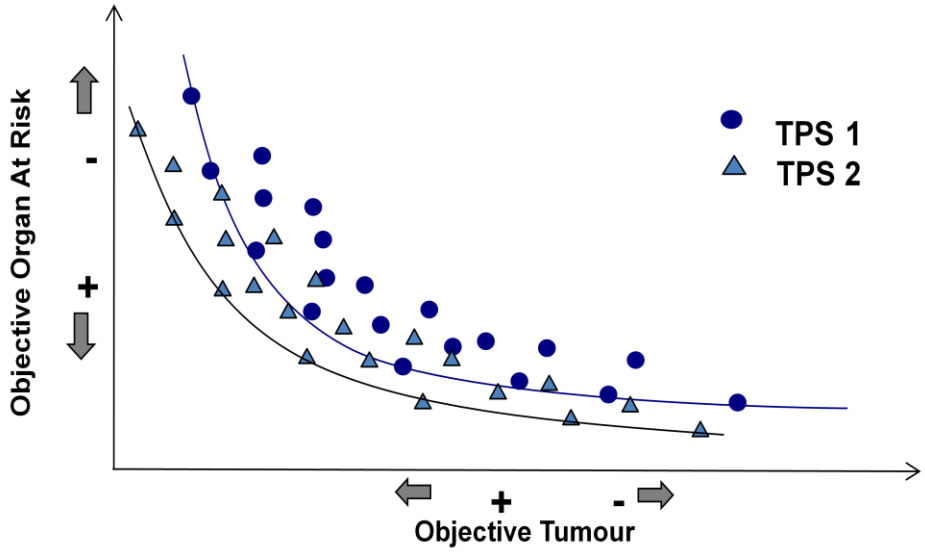

Figure 2: The figure shows a number of objective values for the tumour and for an organ at risk. Every point represents a treatment plan generated. Plans from two different treatment planning systems are plotted in the same diagram. The points on the solid lines are Pareto optimal solutions and lie on the Pareto front. For this fictitious case, TPS 2 is superior to TPS 1.

1.6 The Tomo Therapy Hi-Art system®

The Tomo Therapy Hi-Art system® is different to SIMRT and will therefore be summarized in this section. Tomo Therapy has a linear accelerator producing an x-ray beam of 6MV. The accelerator is rotated around the patient in a ring gantry. The x-ray beam is collimated to a fan beam geometry with a width of 40cm and variable thickness. Tungsten jaws are used as collimators. The fan beam thickness has three different options, 1, 2.5 and 5 cm. Below the collimators there is a binary MLC with 64 leaves. Each leaf can either be open or closed.

The treatment planning in Tomo planning station starts of as for SIMRT, by assigning DVOs. Specific parameters for Tomo are, collimator width pitch and maximum modulation factor. The pitch is the couch movement during a rotation of the accelerator. The modulation factor is the ratio of maximum leaf opening time to the mean leaf opening time. The modulation factor is a tool to control the modulation and thereby the treatment time. Beamlet doses are pre-calculated to speed up the optimization. For Tomo Therapy the MLC leaves are incorporated in the optimization and no segmentation is needed[23, 34].

1.7 Purpose

The purpose of this work was to explore the possibility to compare treatment-planning and treatment-delivery systems for IMRT using a more objective approach. The approach investigated was the Pareto front concept. An additional aim was to adequately compare three different IMRT treatment planning and delivery systems, Oncentra Masterplan (OMP) (Nucletron B.V.), Eclipse (Varian Medical Systems) and TomoTherapy (Tomotherapy inc.), using the Pareto front approach.

2 Materials and Methods

2.1 The cases

Three previously treated head and neck cases were used in the study. The prescribed dose was 68 Gy to the primary planning target volume (PTV T) for case 1 and 66 Gy for case 2 and 3, delivered in 2 Gy fractions. The clinical cases also had outlined elective target volumes (PTV E) and positive nodes (PTV N). The dose to The PTV E for case 1 was prescribed to 50 Gy. For case 2 and 3 there was two PTV Es prescribe to 50 and 60 Gy. The PTV N for all cases should be given the same dose as the PTV T.

The selection criteria for the cases were overlapping of at least one of the target volumes and one of the parotid glands. As a result of this overlap it is expected to be a conflict or trade-off in the optimization between the overlapping structures. The patients were treated at different sites and therefore the gantry angles and photon energies were decided to be the same for Eclipse and OMP. More details on the cases are given in table 1.

Table 1. Case specific information

Case	Diagnose	Prescribed dose [Gy]	PTV [cm2]	Parotid [cm2]	Overlap [cm2]	Overlap [% of parotid]
1	Oropharynx	68	268	24.8	0.2	0.8
2	Oropharynx	66	117	24.5	0.4	1.6
3	Oropharynx	66	95	22.2	6.4	28.8

2.2 Generating the plans

The treatment plans were generated roughly in the same manner for all the systems. For every case one plan was made as good as possible regarding target coverage. All the restrictions to OARs, except for the overlapping parotid gland, were fulfilled according to the DAHANCA protocol [3]. Based on this initial plan the importance of the overlapping parotid gland was varied and several plans were made. The target coverage is expected to decrease as the parotid importance is increased.

Some details are a bit different between the systems. The differences are described later in this thesis. The plans were evaluated in two steps. The first step was the evaluation of critical organs according to DAHANCA[3]. If the plan fulfilled the restrictions, the Pareto optimality was evaluated. All the parameters used in the optimization are presented in the appendix.

2.2.1 OMP

In OMP DVOs for all structures were defined according to the prescribed dose and dose restrictions. Overlapping structures were subtracted so no dose is "stolen" from the target. For example if the PTV and the parotid gland were overlapping the overlapping region was subtracted from the parotid. This resulted in a new structure with no overlap. A DVO was applied to this structure instead of the whole parotid. In order to reduce hot spots outside the PTV a region of interest (ROI) was made containing all the normal tissue. The normal tissue ROI was made by subtracting the PTVs from the outlined body with a margin.

The plans in OMP were generated for an Elekta Synergy accelerator[1] using step & shoot technique. The maximum number of segments, minimum segment size and minimum number of open leaf pairs are parameters that were set before starting the optimization. OMP uses what is called direct step and shoot meaning that the limitations of the MLC are accounted for already in the optimization. In OMP maximum number of iterations for the optimization is set. in this study 40 iterations were used. This number is the one used in the clinic. After the optimization a final dose calculation was made. In this study the dose calculation in OMP is made using Pencil beam convolution.

First a treatment plan with no DVO for the overlapping parotid gland was made. After receiving a satisfying PTV coverage, the importance of the parotid was systematically increased lowering the parotid mean dose. All the plans were made with gantry angle optimization.

2.2.2 Eclipse

The optimization process in Eclipse begins with assigning a DVO only to the PTV and the Normal Tissue Objective Parameters (NTOP)[25]. The NTOP is a built in structure reducing the dose to normal tissue with a margin to the PTV. After receiving a satisfying coverage a DVO for the overlapping parotid gland is added. Just like in OMP only the parotid outside the target is used in the optimization. Because the NTOP is keeping the dose low to normal tissue it is not always necessary to add objectives to other critical organs. The importance of the parotid gland is varied in the same manner as for OMP.

In Eclipse the objectives can be changed during the optimization. Therefore the importance is stepwise increase to the chosen level. For example if the desired parotid importance is 100 it is reached by starting with 10 and running a number of iterations. Then the importance is increased to 20 and so on until 100 is reached.

The optimization is ceased manually when the objective function reaches a plateau. After the optimization segmentation is made. In Eclipse the segmentation generated a dynamic MLC sequence. The final dose is calculated using a pencil beam convolution. All plans were made with gantry angle optimization.

2.2.3 TomoTherapy

In TomoTherapy planning there are two different weighting factors for every DVO available. One called importance is a ranking of the ROIs. The other is called penalty and is a max or min

[1] ElektaOncology Systems, Sweden

dose weight. Every ROI that is used in the optimization must have a max dose objective and a volume objective. These two have separate penalties[34].

In TomoTherapy optimization the overlapping structures are handled automatically. When two structures overlap the one with highest rank is assigned all the overlapping voxels. A target volume is always ranked higher than an OAR. This means that no help structures are needed like in the case with OMP and Eclipse.

The plans were generated in the same manner as in Eclipse by stepwise increasing the importance for the parotid gland to the desired number. The optimization is stopped when no change between the iterations can be seen. TomoTherapy optimizer is taking the MLC into account and no subsequent segmentation is necessary.

2.3 Pareto fronts based on under dosage

All the treatment plans fulfilling the dose restrictions according to clinical protocol were plotted in a Pareto diagram. The average dose for the overlapping parotid gland was plotted as a function of the underdosed volume of the PTV. The PTV plotted was the one with the largest overlap hence the one involved in the trade-off. The underdosed volume was defined as the volume receiving less than 95% of the prescribed dose ($V_{PTV,D<95\%}$). The averaged dose and the under-dosed volume was evaluated from the dose volume histograms (DVH) for each plan.

What in this thesis is called a Pareto front is set of plans representing the Pareto front. About twenty plans were made to get a sample of the Pareto front for each system. The points not contributing to the front were discarded. This step is later on referred to as sorting.

2.4 Pareto fronts based on radiobiology

In this section the purpose was to investigate the possibility to compare Pareto fronts based on radiobiological measures such as the NTCP and TCP. This was made for OMP and Eclipse. At this stage the TomoTherapy could not be evaluated with the radiobiological model.

The normal tissue complication probability (NTCP) for the overlapping parotid gland was plotted as a function of the tumour control probability (TCP) for the target. The NTCP and TCP values were calculated by using the Matlab based program by Gay and Niemierko[35]. This model is based on equivalent uniform dose (EUD)[36]. The parameters used were taken from the work by Eisbruch et al[6]. These parameters are for the end point, less than 25% of the preradiation saliva production one year after the radiation therapy. More details of the model and the parameters used are presented in the appendix.

In the plot the points are not sorted as for the under dosage Pareto fronts (figure 9 and10). The TCP axis is reversed starting at 100% and decreasing. This makes the diagram easier to interpret.

3 Results

3.1 Pareto fronts based on underdosed PTV volume

The Pareto fronts generated with the three different TPSs for case 1 are plotted in the same diagram, (Figure 3). The TomoTherapy front is situated below and to the left of the other fronts indicating that TomoTherapy is able to produce superior plans compared to the standard IMRT systems. The Eclipse Pareto front has better target coverage than OMP for the low priority region (were the priority of the parotid gland is zero or very small). In this low priority regionfor the parotid the coverage of the Eclipse and TomoTherapy are almost the same. The Eclipse front, however, loses coverage faster as the parotid priority is increased and approaches the same coverage as the OMP front. The solid line in figure 3 is marking the average parotid dose of 26 Gy. The three systems reach the 26 Gy level at different under dosage of the PTV. The TomoTherapy is again superior to OMP and Eclipse by reaching 26 Gy to the parotid gland at about 2% under dosage. The eclipse and OMP fronts cross the 26 Gy line at about 4.5% under dosage.

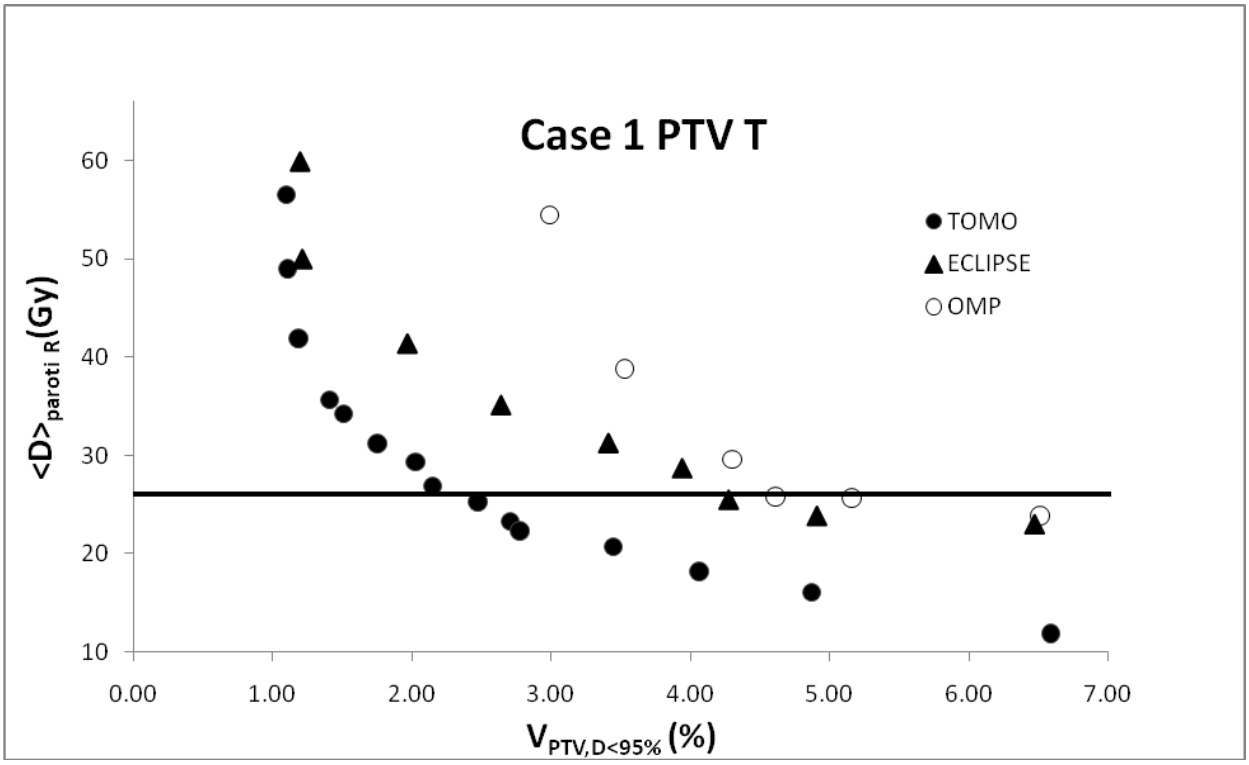

Figure 3: The figure shows the average dose to the right parotid gland as a function of the underdosed volume of the PTV T for case 1. The filled circles represent TomoTherapy, the triangles represent Eclipse and the open circles represent OMP.

For case 2 the same tendencies are present as in case 1 and shown in figure 3. The TomoTherapy front is again below the OMP and Eclipse fronts. For the low priority region Eclipse and TomoTherapy have the same target coverage. As for case 1 the target coverage decreases faster for the Eclipse front and once again approches the coverage of OMP. For this case the

TomoTherapy front reaches the 26Gy level at about 0.6% under-dosage which may be clinically accepted. The OMP and Eclipse fronts reach the 26 Gy line at 2 and 2.5% underdosage, respectivly. All the systems perform considerably better for case 2 compared to case 1.

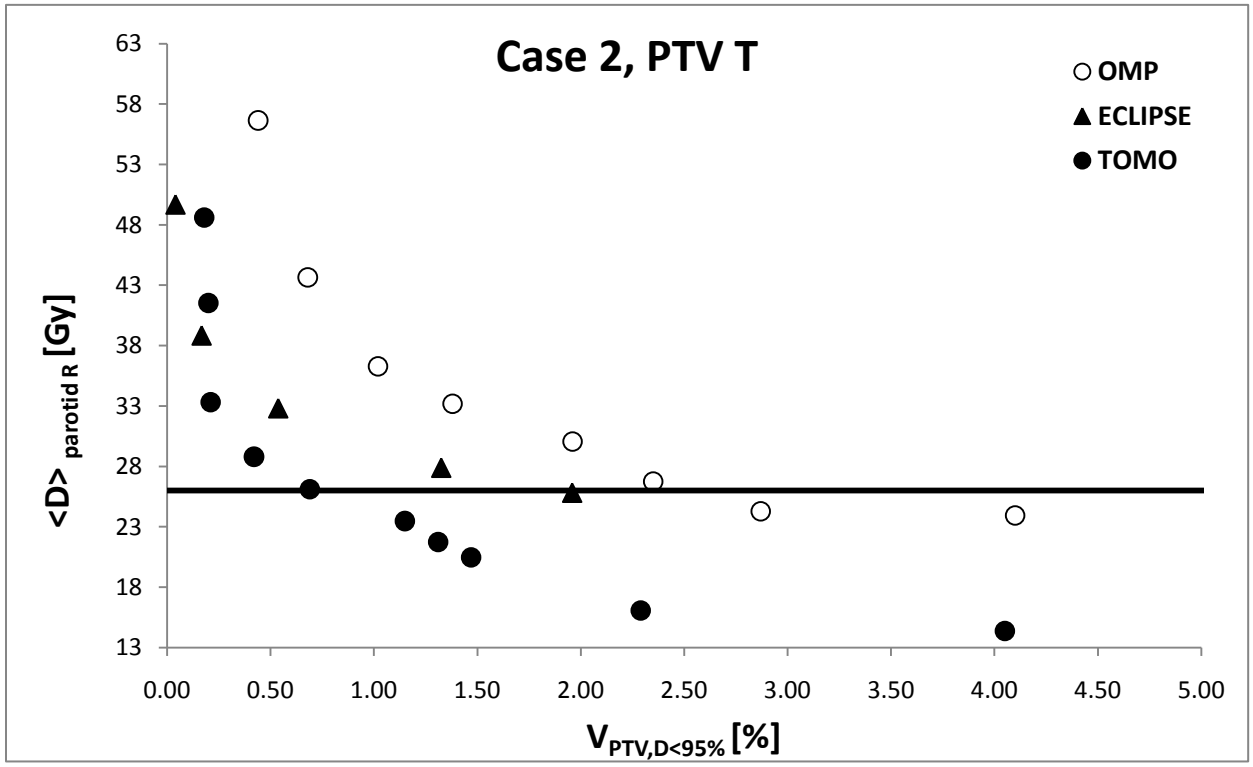

Figure 4: The figure shows the average dose to the right parotid gland as a function of the underdosed volume for the PTV T for case 2. The filled circles represent TomoTherapy, the triangles represent Eclipse and the open circles represent OMP.

For case 3 all the fronts loose target coverage very rapidly as the parotid importance is increased (figure 5). The OMP Pareto front reaches the 26Gy level at about 9% under-dosage. The Tomo Therapy and Eclipse fronts do not reach this level for the studied under-dosage interval. Note that the x axis in figure x goes up to 12%. Because of the similar Pareto fronts for all systems the other PTVs for case 3 were evaluated in the same manner.

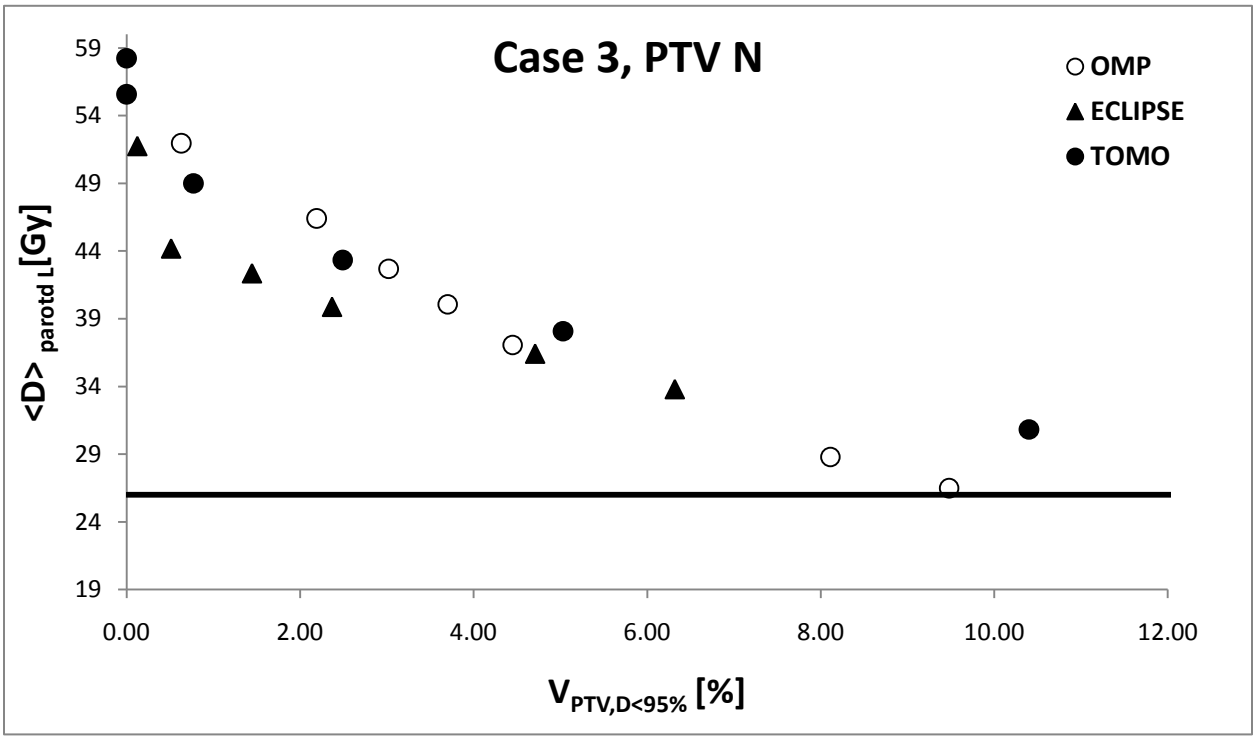

Figure 5: The figure shows the average dose to the left parotid gland as a function of the underdosed volume for the PTV N for case 3. The filled circles represent TomoTherapy, the triangles represent Eclipse and the open circles represent OMP.

The Pareto fronts for PTV T and E are shown in figure 6-8. The TomoTherapy Pareto front shows no trade-off for these PTVs. For eclipse there is little trade off for PTV T. OMP has a trade-off for all PTVs. Note that the underdosed volume is small for the PTV T and the two PTV Es even for OMP.

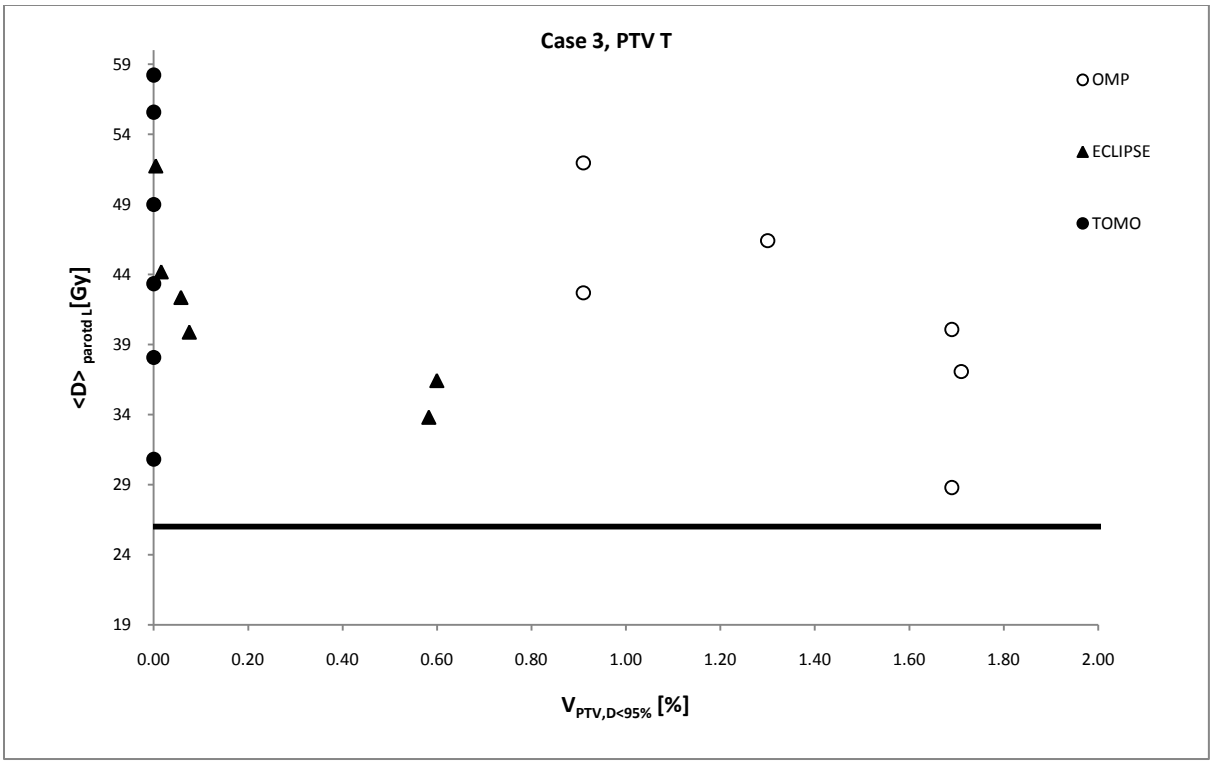

Figure 6: The figure shows the average dose to the left parotid gland as a function of the underdosed volume of the PTV T for case 3. The filled circles represent TomoTherapy, the triangles represent Eclipse and the open circles represent OMP.

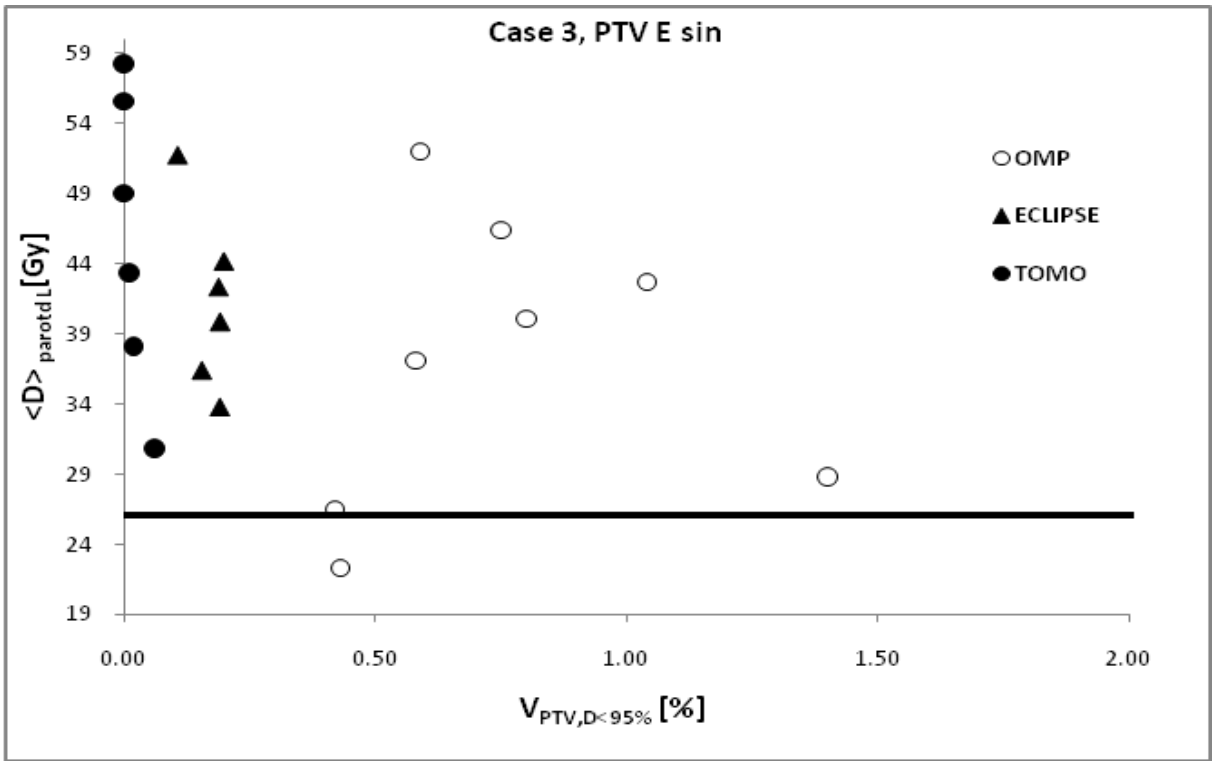

Figure 7: The figure shows the average dose to the left parotid gland as a function of the underdosed volume of the PTV E sin for case 3. The filled circles represent TomoTherapy, the triangles represent Eclipse and the open circles represent OMP.

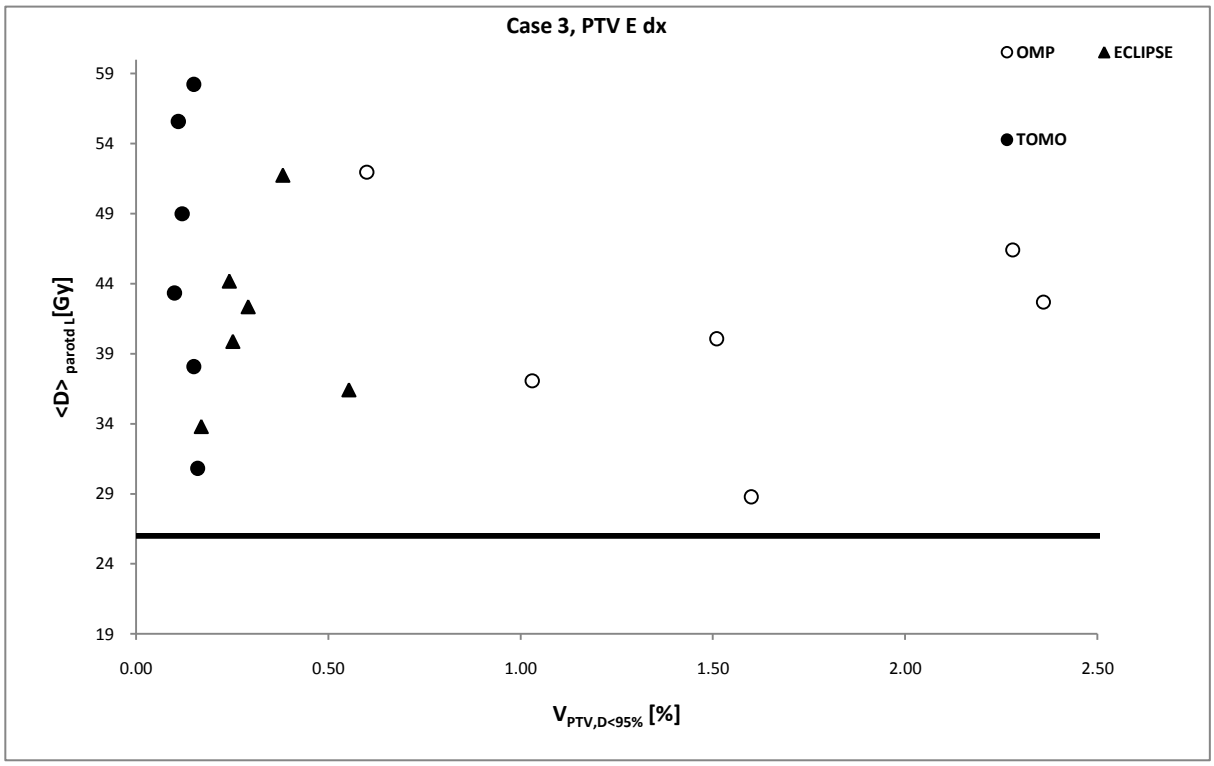

Figure 8: The figure shows the average dose to the left parotid gland as a function of the underdosed volume of the PTV E dx for case 3. The filled circles represent TomoTherapy, the triangles represent Eclipse and the open circles represent OMP.

3.2 Pareto fronts based on TCP and NTCP

A biological evaluation of the treatment plans generated for case 2 and case 3 is presented in this section. The NTCP is shown as a function of TCP for Eclipse and OMP, calculated with angle optimized beams. The set of plans from Eclipse have a more front like shape compared to OMP. For case 2 (figure 9) OMP has larger TCP than Eclipse. Eclipse with optimized angles reaches a TCP of 85% without increasing the NTCP. This TCP value for OMP is about 88%.

The set of treatment plans generated for case 3 (figure 10) are Pareto front shaped for all the systems. Neither of the systems reaches higher TCP than 85%. The NTCP Rapidly increases at this TCP value. For case 3 the two systems are more alike compared to case 2.

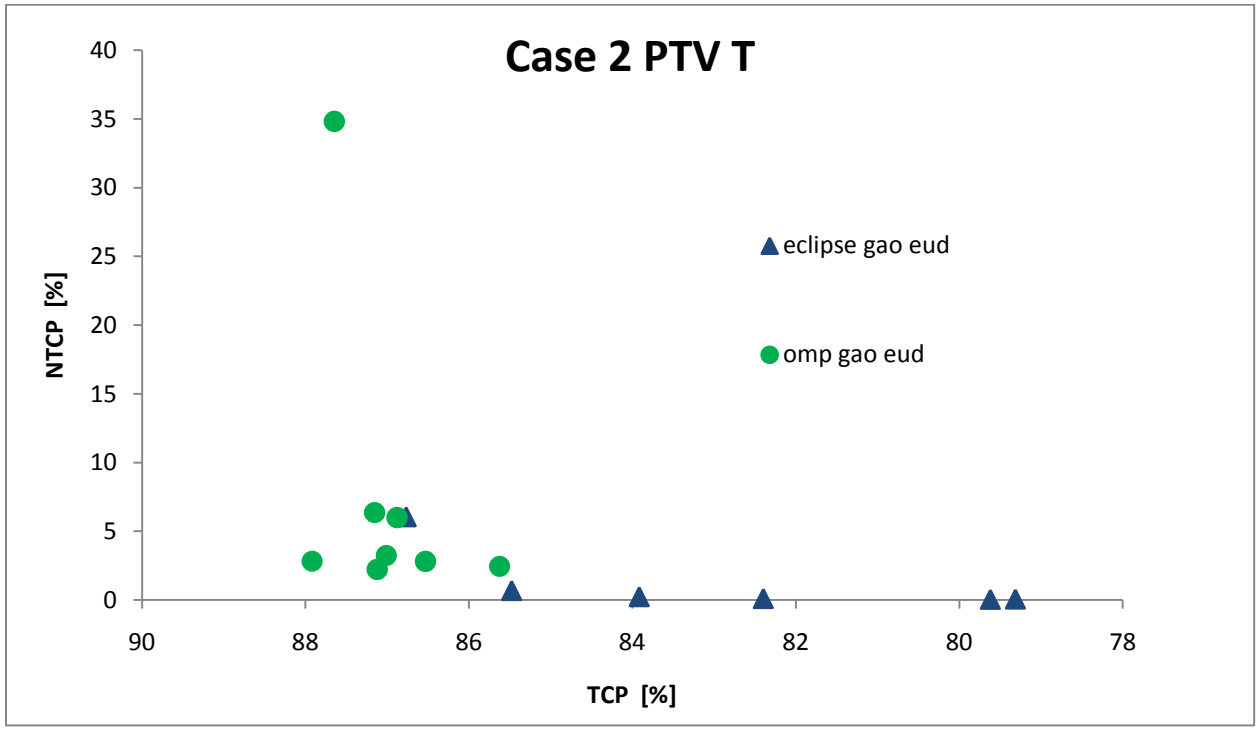

Figure 9: The figure shows the NTCP for the right parotid gland as a function of the TCP for the PTV T for case 2. The blue triangles represent Eclipse and the green circles represent OMP. Note that the x axis is reversed.

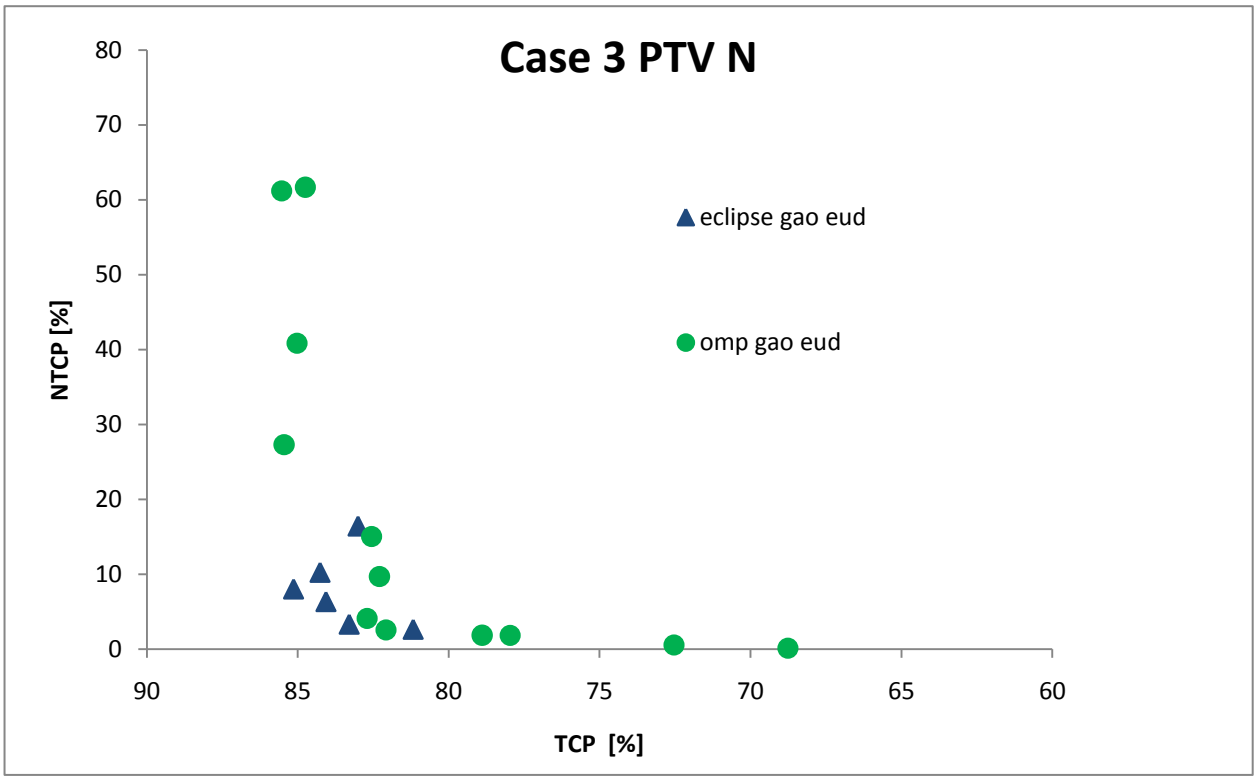

Figure 10: The figure shows the NTCP for the left parotid gland as a function of the TCP for the PTV N for case 3. The blue triangles represent Eclipse and the green circles represent OMP. Note that the x axis is reversed.

4 Discussion and Conclusions

The Pareto fronts from the three systems were separated indicating that the systems performed differently for the same case. The tendencies for the trade-off were the same for case 1 and 2. The TomoTherapy Pareto front was situated below the Eclipse and OMP front indicating a better ability to spare the parotid gland while maintaining a small loss in target coverage. The Eclipse fronts starts with almost the same target coverage as OMP and loses coverage as the parotid is spared. The OMP fronts starts with higher under dosage than Eclipse and Tomo but the decrease is not as rapid as the one for Eclipse. This may be because eclipse uses a dynamic delivery giving better target coverage. The step and shot delivery can block the parotid gland by using segments to a higher extend. For case 3 all systems performed equally bad. This is because of the large overlap between the parotid gland and the target volume.

All the plans generated with TomoTherapy and Eclipse systems followed the Pareto front for the system. This was not the case for OMP. The plans generated with OMP had to be sorted to present a Pareto front. This required a large number of plans made by varying the parotid importance in smaller steps. The non Pareto optimal plans from OMP may be a result of the way the optimizer works. In OMP all parameters and DVOs are set and the optimization runs for a preset number of iterations. The number of iterations used in this study was the one used clinically at the Lund university hospital. Because of this the optimizer may not always reach a plateau. Letting the optimization run for more iterations it can reach the plateau but then the plans get more complex and cannot be delivered. The optimization in TomoTherapy and Eclipse is ceased when the plateau is reached.

For case 2 and 3 a radiobiological approach was also investigated as a comparison method. The biological model is using a different endpoint than total mouth dryness. The biological models can perhaps give prediction of the treatment outcome. The results from the biological evaluation indicates a threshold were the TCP cannot be improved. At this threshold level the NTCP is rapidly increasing. To a certain TCP level the NTCP is fairly low. This means that the parotid gland can be spared without losing TCP.

The Pareto fronts made based on NTCP and TCP were not sorted so the non Pareto optimal plans can be seen as well. There were non Pareto optimal fronts for all the systems. This can be because the optimization was not based on TCP and NTCP. The biological approach needs to med further investigated but seems promising.

Comparing Pareto fronts instead of single plans gives a wider picture of the system. The whole range from low to high OAR priority can be evaluated at the same time. If two single plans are compared the position on the Pareto front is missed. The selected plan may not even be Pareto optimal.

The Pareto fronts also give information that is not accessible in a DVH. This can be, as seen in figure 4 and 5, the sparing of the parotid without losing target coverage.

The results clearly indicate that the approach of using Pareto fronts for different systems is a feasible way to compare different methods and technologies for advanced radiotherapy. For the particular cases studied, TomoTherapy seems to be superior to OMP and Eclipse regarding target coverage and sparing of the parotid gland.

5 Future Aspects

To make the Pareto front based comparison more usable an automatic generation of plans is desired. Today the plan generating process is time consuming. Efforts have been made to make plans automatically based on Pareto fronts but these studies use in house develop optimizers [30, 37]. Because of this it cannot be used to compare commercial systems. Other treatment sites would make the comparison more broad.

The radiobiological approach needs to be further investigated to include TomoTherapy as well. Other models and parameters may be tested. Endpoints other than xerostomia may also be investigated.

A quantification of the Pareto fronts would make the comparison more powerful. This would not only give a picture of the system but also information of the trade-off for each case. Area under the curve (AUC) may be a way to make this quantification. Using AUC would give a number for every Pareto front. Lower numbers would represent better OAR sparing for the same target coverage.

It would also be interesting to compare other TPSs and delivery systems. A comparison between TomoTherapy and other rotational techniques would be exciting.

6 Acknowledgments

I would like to thank all the people involved in this work. At first I thank my colleague and friend Maria Thor, who provided me with the Eclipse plans from Herlev.

I would also like to thank my supervisors in Lund, Per Engström, Crister Ceberg and Tommy Knöös, for all there help and guidance during the project.

My supervisors in Herlev, Anna Karlsson and Claus Behrens deserve big thanks for all the valuable ideas during meetings and my visits to Herlev.

I would like to acknowledge the John and Augusta Persson's foundation for financinge my atendencce at the 10th Biennial ESTRO Conference on Physics and Radiation Technology for Clinical Radiotherapy, where I presented part of this study.

I would like to Thank Per Nilsson for helping me with the biological models. And last but not least I thank Kristoffer Petersson for the good discussions improving the study.

7 References

1. Haddad, R.I. and D.M. Shin, *Recent advances in head and neck cancer.* N Engl J Med, 2008. **359**(11): p. 1143-54.
2. Burnet, N.G., et al., *Improving cancer outcomes through radiotherapy. Lack of UK radiotherapy resources prejudices cancer outcomes.* BMJ, 2000. **320**(7229): p. 198-9.
3. DAHANCA, *Retningsliner for strålbehandling af hoved-hals cancer (Cavum Oris, Pharynx, Larynx) inklusiv IMRT vejledning.* http://www.dahanca.dk/get_media_file.php?mediaid=57, , 2004.
4. Tome, W.A. and J.F. Fowler, *On cold spots in tumor subvolumes.* Med Phys, 2002. **29**(7): p. 1590-8.
5. Cooper, J.S., et al., *Late effects of radiation therapy in the head and neck region.* Int J Radiat Oncol Biol Phys, 1995. **31**(5): p. 1141-64.
6. Eisbruch, A., et al., *Dose, volume, and function relationships in parotid salivary glands following conformal and intensity-modulated irradiation of head and neck cancer.* Int J Radiat Oncol Biol Phys, 1999. **45**(3): p. 577-87.
7. Bortfeld, T., *IMRT: a review and preview.* Phys Med Biol, 2006. **51**(13): p. R363-79.
8. Webb, S., *The physical basis of IMRT and inverse planning.* Br J Radiol, 2003. **76**(910): p. 678-89.
9. Brahme, A., J.E. Roos, and I. Lax, *Solution of an integral equation encountered in rotation therapy.* Phys Med Biol, 1982. **27**(10): p. 1221-9.
10. Vergeer, M.R., et al., *Intensity-modulated radiotherapy reduces radiation-induced morbidity and improves health-related quality of life: results of a nonrandomized prospective study using a standardized follow-up program.* Int J Radiat Oncol Biol Phys, 2009. **74**(1): p. 1-8.
11. Ahmed, M., et al., *Reducing the risk of xerostomia and mandibular osteoradionecrosis: the potential benefits of intensity modulated radiotherapy in advanced oral cavity carcinoma.* Med Dosim, 2009. **34**(3): p. 217-24.
12. Cozzi, L., et al., *Three-dimensional conformal vs. intensity-modulated radiotherapy in head-and-neck cancer patients: comparative analysis of dosimetric and technical parameters.* Int J Radiat Oncol Biol Phys, 2004. **58**(2): p. 617-24.
13. Bhide, S., et al., *Intensity modulated radiotherapy improves target coverage and parotid gland sparing when delivering total mucosal irradiation in patients with squamous cell carcinoma of head and neck of unknown primary site.* Med Dosim, 2007. **32**(3): p. 188-95.
14. Wu, Q., et al., *The potential for sparing of parotids and escalation of biologically effective dose with intensity-modulated radiation treatments of head and neck cancers: a treatment design study.* Int J Radiat Oncol Biol Phys, 2000. **46**(1): p. 195-205.
15. van Rij, C.M., et al., *Parotid gland sparing IMRT for head and neck cancer improves xerostomia related quality of life.* Radiat Oncol, 2008. **3**: p. 41.
16. Verbakel, W.F., et al., *Volumetric intensity-modulated arc therapy vs. conventional IMRT in head-and-neck cancer: a comparative planning and dosimetric study.* Int J Radiat Oncol Biol Phys, 2009. **74**(1): p. 252-9.
17. Moon, S.H., et al., *Dosimetric comparison of four different external beam partial breast irradiation techniques: three-dimensional conformal radiotherapy, intensity-modulated*

radiotherapy, helical tomotherapy, and proton beam therapy. Radiother Oncol, 2009. **90**(1): p. 66-73.
18. Sheng, K., et al., *A dosimetric comparison of non-coplanar IMRT versus Helical Tomotherapy for nasal cavity and paranasal sinus cancer.* Radiother Oncol, 2007. **82**(2): p. 174-8.
19. Longobardi, B., et al., *Comparing 3DCRT and inversely optimized IMRT planning for head and neck cancer: equivalence between step-and-shoot and sliding window techniques.* Radiother Oncol, 2005. **77**(2): p. 148-56.
20. Mavroidis, P., et al., *Treatment plan comparison between helical tomotherapy and MLC-based IMRT using radiobiological measures.* Phys Med Biol, 2007. **52**(13): p. 3817-36.
21. Lian, J., et al., *Assessment of extended-field radiotherapy for stage IIIC endometrial cancer using three-dimensional conformal radiotherapy, intensity-modulated radiotherapy, and helical tomotherapy.* Int J Radiat Oncol Biol Phys, 2008. **70**(3): p. 935-43.
22. Shi, C., J. Penagaricano, and N. Papanikolaou, *Comparison of IMRT treatment plans between linac and helical tomotherapy based on integral dose and inhomogeneity index.* Med Dosim, 2008. **33**(3): p. 215-21.
23. Peter Metcalfe, Peter Hoban , ,Tomas Kron, *The Physics of Radiotherapy X-rays and Electrons*. 2007, Madison: Medical Physics Publishing.
24. Jatinder R. Palta , T.Rockwell Mackie, ed. *Intensity - Modulated Radiation Therapy*. Vol. 1. 2003, Medical Physics Publishing: Madison. 888.
25. *Varian Medical systems, Eclipse IMRT external beam planning system version 8.5.0, Copyright © 2008*
26. *Oncentra MasterPlan version 3.1 - Physics and Algorithms*. 2008.
27. Boyd, S., Vadenberghe,L, *Convex Optimization*. 2004, Cambridge: CAMBRIDGE UNIVERSITY PRESS.
28. Hong, T.S., et al., *Multicriteria optimization in intensity-modulated radiation therapy treatment planning for locally advanced cancer of the pancreatic head.* Int J Radiat Oncol Biol Phys, 2008. **72**(4): p. 1208-14.
29. Ottosson, R.O., et al., *The feasibility of using Pareto fronts for comparison of treatment planning systems and delivery techniques.* Acta Oncol, 2009. **48**(2): p. 233-7.
30. Monz, M., et al., *Pareto navigation: algorithmic foundation of interactive multi-criteria IMRT planning.* Phys Med Biol, 2008. **53**(4): p. 985-98.
31. Craft, D., T. Halabi, and T. Bortfeld, *Exploration of tradeoffs in intensity-modulated radiotherapy.* Phys Med Biol, 2005. **50**(24): p. 5857-68.
32. Hoffmann, A.L., et al., *Derivative-free generation and interpolation of convex Pareto optimal IMRT plans.* Phys Med Biol, 2006. **51**(24): p. 6349-69.
33. Hoffmann, A.L., et al., *Convex reformulation of biologically-based multi-criteria intensity-modulated radiation therapy optimization including fractionation effects.* Phys Med Biol, 2008. **53**(22): p. 6345-62.
34. *Tomo- Planning Guide version 3.x*. 2008.
35. Gay, H.A. and A. Niemierko, *A free program for calculating EUD-based NTCP and TCP in external beam radiotherapy.* Phys Med, 2007. **23**(3-4): p. 115-25.
36. Niemierko, A., *Reporting and analyzing dose distributions: a concept of equivalent uniform dose.* Med Phys, 1997. **24**(1): p. 103-10.

37. Thieke, C., et al., *A new concept for interactive radiotherapy planning with multicriteria optimization: first clinical evaluation.* Radiother Oncol, 2007. **85**(2): p. 292-8.

Appendix

1 Planning parameters

Table 2. Specific parameters for Oncentra MasterPlan

Case	Maximum number of segments	Min segment size [cm2] OMP	Min number of open leaf pairs	Min number of MU/ segment
1	120	5	4	3
2	120	5	4	3
3	120	5	4	3

Table 3. Specific parameters for TomoTherapy Hi-art® system

Case	pitch	Jaw [cm]	Modulation Factor
1	0.3	2.5	3
2	0.3	2.5	3
3	0.3	2.5	3

Table 4. Specific parameters for Eclipse IMRT external beam planning system

Case	Smoothing [x, y] Eclipse
1	60
2	60
3	60

2 EUD-based NTCP and TCP

EUD-based mathematical is simple because it is based on two equations. It is also practical because the same model is used for both TCP and NTCP calculations. The EUD is calculated by the following phenomenological model.

$$EUD = \left(\sum_{i=1} (v_i D_i^a)\right)^{\frac{1}{a}} \qquad (5)$$

a is a unitless model parameter that is specified for either normal tissue or tumour structures. v_i is the *i*th partial volume element receiving the dose D_i in Gy. This EUD model can be used for both normal tissue and tumour structures. For normal tissue the EUD represents the uniform dose that leads to the same probability of injury as the non uniform dose distribution investigated. The model used for calculating the NTCP is as follows:

$$NTCP = \frac{1}{1 + \left(\frac{TD_{50}}{EUD}\right)^{4\gamma 50}} \qquad (6)$$

The TD_{50} is the tolerance dose for 50% complication rate. The γ_{50} is a model parameter that describes the slope of the dose response curve for the tissue. For TCP calculation the following model is used:

$$TCP = \frac{1}{1 + \left(\frac{TDC_{50}}{EUD}\right)^{4\gamma_{50}}} \qquad (7)$$

The TDC_{50} is the dose to control 50% of the tumours when irradiated homogeneously. By choosing the right model parameters the model can be fitted for the desired structure[35], in this study the parotid gland and oropharynx cancer. The parameters used are presented in table 5.

Table 5: The parameters used for the radiobiological model.

	a	TD_{50}/TDC_{50} [Gy]	γ_{50}
NTCP parotid	1	28.4	2.2
TCP T_1-T_2 tumours	-13	57.0	2.7
TCP T_3-T_4 tumours	-13	70.5	2.5